Ubiquitinated TDP-43 in Frontotemporal Lobar Degeneration and Amyotrophic Lateral Sclerosis

Manuela Neumann,[1,11]* Deepak M. Sampathu,[1]* Linda K. Kwong,[1]* Adam C. Truax,[1] Matthew C. Micsenyi,[1] Thomas T. Chou,[2] Jennifer Bruce,[1] Theresa Schuck,[1] Murray Grossman,[3,4] Christopher M. Clark,[3,4] Leo F. McCluskey,[3] Bruce L. Miller,[6] Eliezer Masliah,[7] Ian R. Mackenzie,[8] Howard Feldman,[9] Wolfgang Feiden,[10] Hans A. Kretzschmar,[11] John Q. Trojanowski,[1,4,5] Virginia M.-Y. Lee[1,4,5]†

Ubiquitin-positive, tau- and α-synuclein–negative inclusions are hallmarks of frontotemporal lobar degeneration with ubiquitin-positive inclusions and amyotrophic lateral sclerosis. Although the identity of the ubiquitinated protein specific to either disorder was unknown, we showed that TDP-43 is the major disease protein in both disorders. Pathologic TDP-43 was hyperphosphorylated, ubiquitinated, and cleaved to generate C-terminal fragments and was recovered only from affected central nervous system regions, including hippocampus, neocortex, and spinal cord. TDP-43 represents the common pathologic substrate linking these neurodegenerative disorders.

Ubiquitination of misfolded proteins that aggregate in the cytoplasm and/or nucleus of central nervous system (CNS) neurons is a key characteristic of neurodegenerative diseases (*1*). Misfolded disease proteins have been identified in many neurodegenerative disorders, but the identities of the ubiquitinated disease protein(s) in UBIs (defined here as ubiquitinated cytoplasmic, nuclear, and neuritic inclusions) in frontotemporal lobar degeneration (FTLD-U), the most common frontotemporal dementia (FTD) (*2*–*5*), and amyotrophic lateral sclerosis (ALS) are enigmatic. FTDs are clinically, genetically, and pathologically heterogeneous, but they are the most common cause of dementia under age 65 after Alzheimer's disease (AD) (*6*, *7*). FTDs present with progressive changes in social, behavioral, and/or language dysfunction (*7*–*9*), and some patients also develop parkinsonism or motor neuron disease (MND) (*2*, *10*). Conversely, ALS, a form of MND, is often associated with FTD (*10*), with UBIs identical to FTLD-U (*6*). Thus, clinical and pathological overlap in FTLD-U and ALS suggest they represent different manifestations of the same neurodegenerative disorder.

More than 30% of FTDs are familial, and many kindreds show linkage to chromosome 17 (*6*, *11*, *12*). However, FTD with parkinsonism linked to chromosome 17 (FTDP-17) usually shows tau pathology caused by pathogenic mutations in the microtubule-associated protein tau gene (*MAPT*) (*13*, *14*), FTDP-17T, but several FTDP-17 families are characterized by UBIs (FTDP-17U) without *MAPT* mutations (*15*–*17*). Recently, mutations in the progranulin gene (*PGRN*) were shown to be pathogenic for FTDP-17U (*11*, *12*). Because PGRN is not incorporated into UBIs in FTDP-17U (*11*, *12*), the FTLD-U disease protein remains to be identified.

On the basis of immunohistochemistry with ubiquitin and novel monoclonal antibodies (mAbs), at least three FTLD-U subtypes (types

[1]Center for Neurodegenerative Disease Research, Department of Pathology and Laboratory Medicine, [2]Department of Pharmacology, [3]Department of Neurology, [4]Alzheimer's Disease Core Center, [5]Institute on Aging, University of Pennsylvania School of Medicine, Philadelphia, PA 19104, USA. [6]Department of Neurology, University of California at San Francisco, CA 94117, USA. [7]Department of Neurosciences, University of California San Diego, School of Medicine, La Jolla, CA 92093, USA. [8]Department of Pathology, [9]Division of Neurology, University of British Columbia, Vancouver, British Columbia V6T 2B5, Canada. [10]Institute for Neuropathology, University of the Saarland, 66421 Homburg, Germany. [11]Center for Neuropathology and Prion Research, Ludwig-Maximilians University, 81377 Munich, Germany.

*These authors contributed equally to this work.
†To whom correspondence should be addressed. E-mail: vmylee@mail.med.upenn.edu

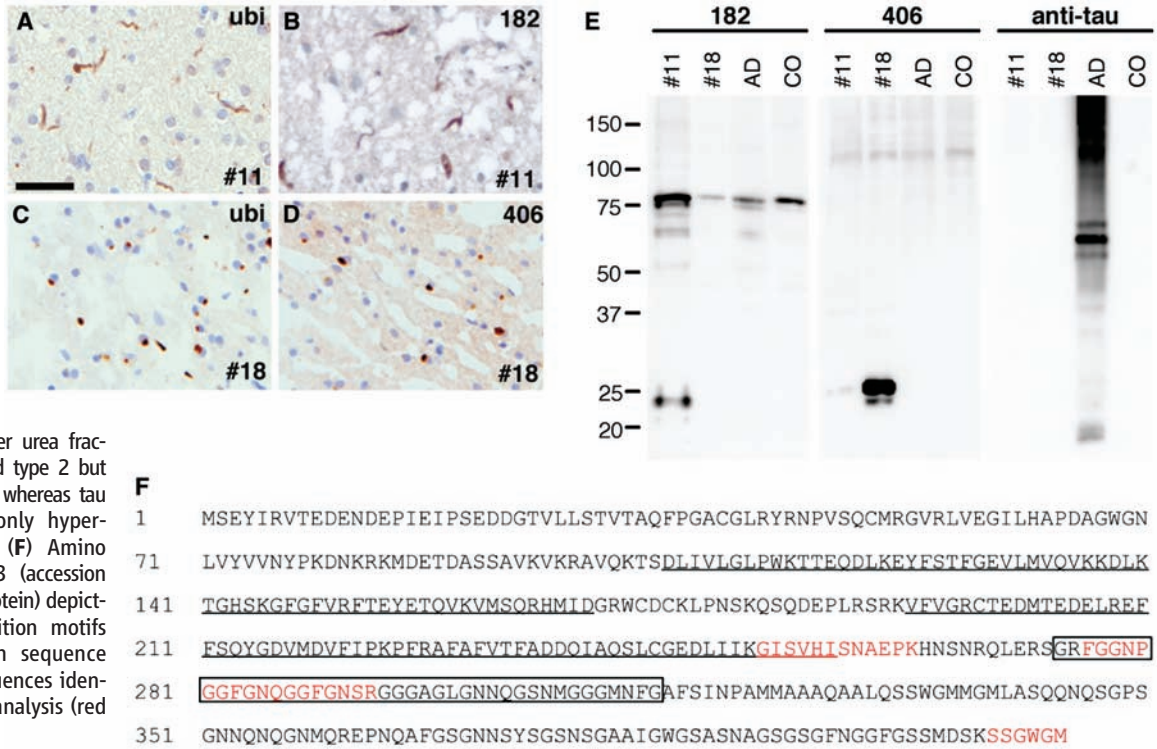

Fig. 1. Identification of TDP-43 as the major disease protein in UBIs of FTLD-U. (**A** to **D**) mAb 182 specifically labeled neuritic UBIs in FTLD-U type 1 [(A) and (B)], whereas mAb 406 immunostained UBIs in FTLD-U type 2 cases [(C) and (D)]. Scale bar in (A) corresponds to 25 μm for (A) to (D). (**E**) mAbs 182 and 406 detected disease-specific bands ~24 kD and ~26 kD, respectively, in frontal gray matter urea fractions of FTLD-U type 1 and type 2 but not in those of AD or CO, whereas tau mAbs T14/46 detected only hyperphosphorylated AD tau. (**F**) Amino acid sequence of TDP-43 (accession no. NP_031401, Entrez Protein) depicting the two RNA-recognition motifs (underlined), glycine-rich sequence (boxed), and peptide sequences identified through LC-MS/MS analysis (red highlights).

1 to 3) have been identified (*18*), suggesting that either different disease proteins or modifications of a single protein could underlie FTLD-U variants. Additional mAbs specific for distinct FTLD-U subtypes were generated (*19*), and mAb 182 was highly specific for UBIs in FTLD-U type 1 (Fig. 1, A and B, and table S1, nos. 1 to 12), whereas mAb 406 specifically labeled UBIs in FTLD-U type 2 cases (Fig. 1, C and D, and table S1, nos. 13 to 26). To further characterize the disease protein(s) recognized by mAbs 182 and 406, we performed immunoblots on urea fractions from FTLD-U types 1 and 2 brains. Notably, mAb 182 recognized an ~24-kD band in the urea fraction of type 1 that was not present in type 2, AD, or normal (CO) brains, whereas mAb 406 detected an ~26-kD band in FTLD-U type 2, but not in type 1, AD, or CO (Fig. 1E). As expected, tau antibodies detected insoluble pathological tau in AD but not in FTLD-U type 1, type 2, or CO (Fig. 1E), and mAbs 182 and 406 did not detect the 24- and 26-kD bands in FTLD-U type 3 and FTDP-17U cases.

To determine the identity of the 24- and 26-kD protein bands recognized by mAbs 182 and 406, respectively, we performed two-dimensional polyacrylamide gel electrophoresis (2D PAGE) immunoblots by using urea fractions from types 1 and 2 brains. MAbs 182 and 406 immunolabeled protein spots ~25 kD with a pI ~ 3.5 (fig. S1, A and C). The same spots were identified on duplicate Coomassie Blue–stained 2D PAGE gels (fig. S1, B and D) and analyzed by liquid chromatography–tandem mass spectrometry (LC-MS/MS). The same three peptides corresponding to amino acid residues 252 to 263, 276 to 293, and 409 to 414 of the TAR-DNA-binding protein 43 (TDP-43) were identified (Fig. 1F). Notably, the 409-414 peptide is at the extreme C terminus of TDP-43, suggesting that both 24- and 26-kD fragments are truncated in the middle of TDP-43 and extend to its C terminus.

The human gene encoding TDP-43 (*TARDP*) on chromosome 1 was cloned and shown to bind a polypyrimidine-rich motif in the HIV transactive response DNA (*20*), but it was later identified independently as part of a complex involved in the splicing of the cystic fibrosis transmembrane conductance regulator gene (*21*). TDP-43 contains two RNA-recognition motifs as well as a glycine-rich C-terminal sequence (*22*) (Fig. 1F) and is widely expressed in tissues, including heart, lung, liver, spleen, kidney, muscle, and brain (*21*). Because the same peptides were recovered from protein spots detected by mAbs 182 and 406, this suggests that both mAbs recognize specific conformations or posttranslational modifications of a C-terminal breakdown and/or cleavage product of TDP-43 unique to FTLD-U type 1 and 2, respectively.

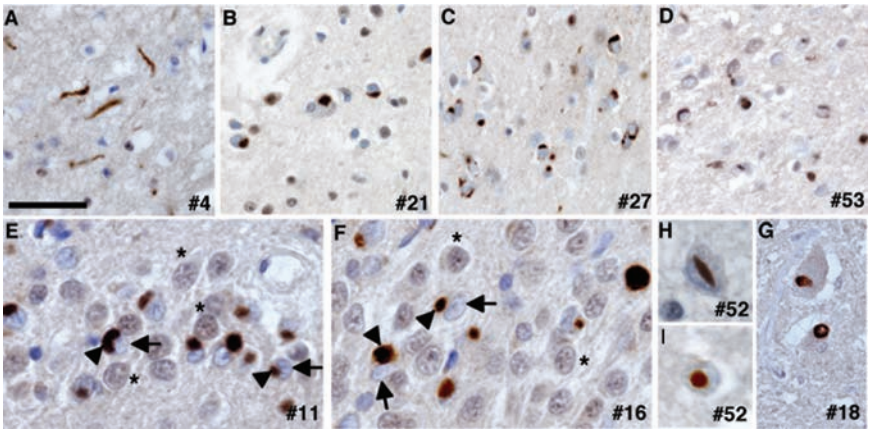

Fig. 2. Spectrum of FTLD-U neuropathology detected by anti–TDP-43. Immunohistochemistry of FTLD-U frontal cortex with anti–TDP-43 reveals robust staining of UBIs in FTLD-U (**A**) type 1, (**B**) type 2, (**C**) type 3, and (**D**) HDDD2. (**E** and **F**) Strong staining of UBIs (arrowheads) in hippocampal dentate granule neurons. Note clearing of nuclear TDP-43 (arrows) in UBI-bearing neurons compared that of with normal neurons (*). TDP-43–positive lentiform (**H**) and round (**G**) intranuclear UBIs in HDDD2 and Lewy body–like round inclusions in motor neurons of spinal cord (**I**). Scale bar in (A) corresponds to 50 μm [(A) to (D) and (G)], 25 μm [(E) and (F)] and 20 μm [(H) and (I)].

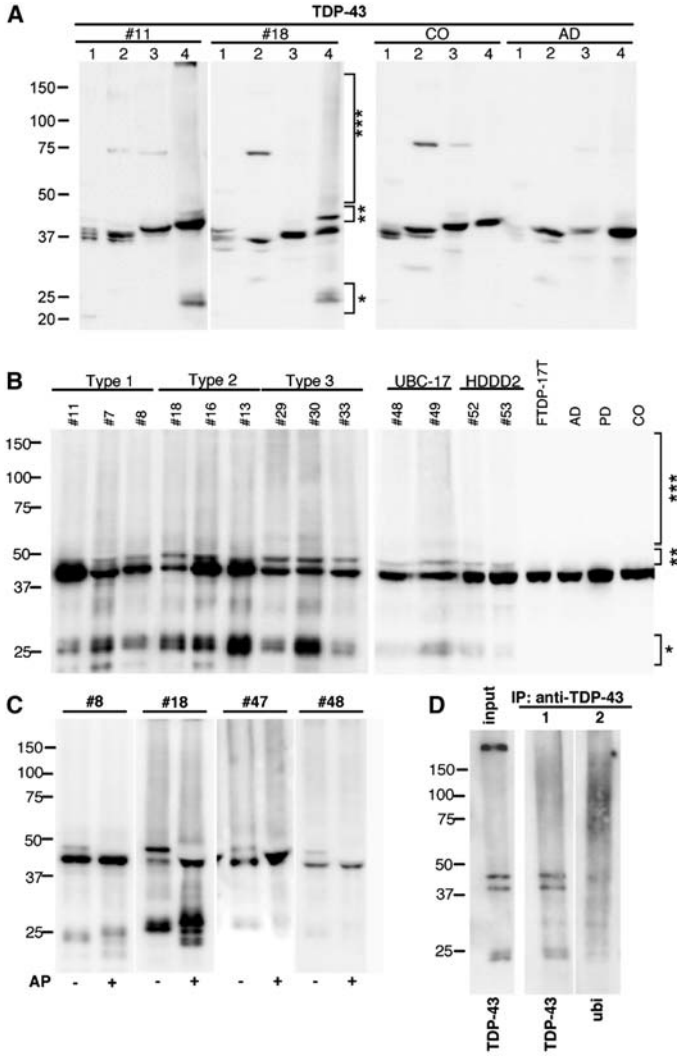

Fig. 3. Biochemical analyses of TDP-43 in sporadic and familial FTLD-U. (**A**) Immunoblots of sequential extracts from frontal cortex of FTLD-U types 1 and 2 with rabbit anti–TDP-43 showed pathologic ~25-kD bands (*), 45-kD bands (**), and high M_r smear (***) in the urea fraction. Lane 1, low salt; 2, high salt with triton x-100; 3, sarkosyl; 4, urea. (**B**) Immunoblots of urea fractions from hippocampal and temporal cortex of FTLD-U types 1 to 3 and frontal cortex of FTDP-17U showed the distinct pathological profile of TDP-43 not present in other neurodegenerative diseases or CO. (**C**) Dephosphorylation of FTLD-U urea extracts collapsed the 45-kD band into the 43-kD band and separated truncated TDP-43 into four immunoreactive ~23- to ~27-kD bands. (**D**) Immunoprecipitation of FTLD-U urea extract with anti–TDP-43 followed by immunoblotting with anti–TDP-43 (lane 2) and ubiquitin (Ub1B4) (lane 3) antibodies revealed that TDP-43 is ubiquitinated.

Double-labeling immunofluorescence studies showed that TDP-43 antibodies (anti–TDP-43) strongly immunolabeled UBIs detected by mAb 182 in FTLD-U type 1 cases and by mAb 406 in FTLD-U type 2 cases (fig. S2, A to F). Surprisingly, anti–TDP-43 robustly labeled UBIs that were not detected by mAbs 182 and 406 in FTLD-U type 3 cases, as well as UBIs in familial FTDP-17U brains (fig. S2, G to L). Anti–TDP-43 detected at least as many UBIs as ubiquitin antibodies or mAbs 182 and 406 in these FTLD-U brains.

Robust anti–TDP-43 staining was observed in affected cortical regions of FTLD-U type 1 (Fig. 2A and fig. S3, A and E), type 2 (Fig. 2B and fig. S3, B and F), and type 3 (Fig. 2C and fig. S3, C and G) cases, with the distinct morphology and distribution pattern characteristic of each of these FTLD-U subtypes (*18*). TDP-43–positive UBIs resembling those described for FTLD-U type 3 were detected in two separate FTDP-17U pedigrees [UBC-17 (*16*) and HDDD2 (*17*)] (Fig. 2D and fig. S3, D and H). Furthermore, strong TDP-43 staining was observed in UBIs of hippocampal dentate granule cells (Fig. 2, E and F) and in intranuclear UBIs characteristic of FTDP-17U cases (Fig. 2, G and H). Notably, TDP-43 was detectable in the nuclei of unaffected neurons but absent in nuclei of neurons with UBIs (asterisks, arrows, and arrowheads in Fig. 2, E and F), suggesting that TDP-43 redistributes from nucleus to cytoplasm in affected neurons. Furthermore, anti–TDP-43 labeled UBIs in the motor neurons of spinal cord and brain stem in FTLD-U cases with and without clinical signs of MND (Fig. 2I). Diagnostic inclusions of other neurodegenerative disorders were uniformly TDP-43–negative (fig. S3, I to T). Thus, TDP-43 is a highly specific disease protein found in neuronal UBIs of all FTLD-U subtypes and FTDP-17U.

To characterize TDP-43 protein biochemically, we sequentially extracted cortical gray matter from FTLD-U and FTDP-17U brains with buffers of increasing strength and analyzed the samples by immunoblot. Whereas full-length TDP-43 protein was present in all soluble and insoluble fractions of FTLD-U type 1 and type 2 as well as AD and CO, a strong labeling of ~25-kD bands similar to those detected by mAbs 182 and 406 was only detectable in the urea fractions of FTLD-U types 1 and 2, respectively (single asterisk in Fig. 3A). Further, a higher ~45-kD band and a high relative molecular mass (M_r) smear were recognized by anti–TDP-43 in the urea fractions of the FTLD-U brains compared with those of AD and CO (double and triple asterisks in Fig. 3A). Analyzing urea fractions extracted from hippocampus or frontal cortex of multiple FTLD-U brains demonstrates that this disease-specific TDP-43 signature was observed in all FTLD-U subtypes and familial FTDP-17U except in unaffected regions (e.g., cerebellum), and it was FTLD-U specific because it was not detected in CO or in other neurodegenerative disorders (e.g., AD and FTDP-17T) (Fig. 3B). Thus, the signature of pathological TDP-43 in FTLD-U includes the presence of C-terminal breakdown and/or cleavage products migrating at ~25 kD, a ~45-kD M_r variant, and a high-M_r TDP-43-immunoreactive smear, although quantities of pathological species of TDP-43 varied, possibly reflecting the extent of UBIs in diverse brain regions of different FTLD-U cases.

To determine what accounts for these disease-specific alterations of TDP-43 and because TDP-43 contains numerous potential phosphorylation sites, we next investigated the phosphorylation state of TDP-43 in FTLD-U. Dephosphorylation of urea fractions of FTLD-U brains showed collapsing of the 45-kD band into a 43-kD band (Fig. 3C) and separated the two C-terminal fragments into at least four distinct TDP-43 immunobands (Fig. 3C). Thus,

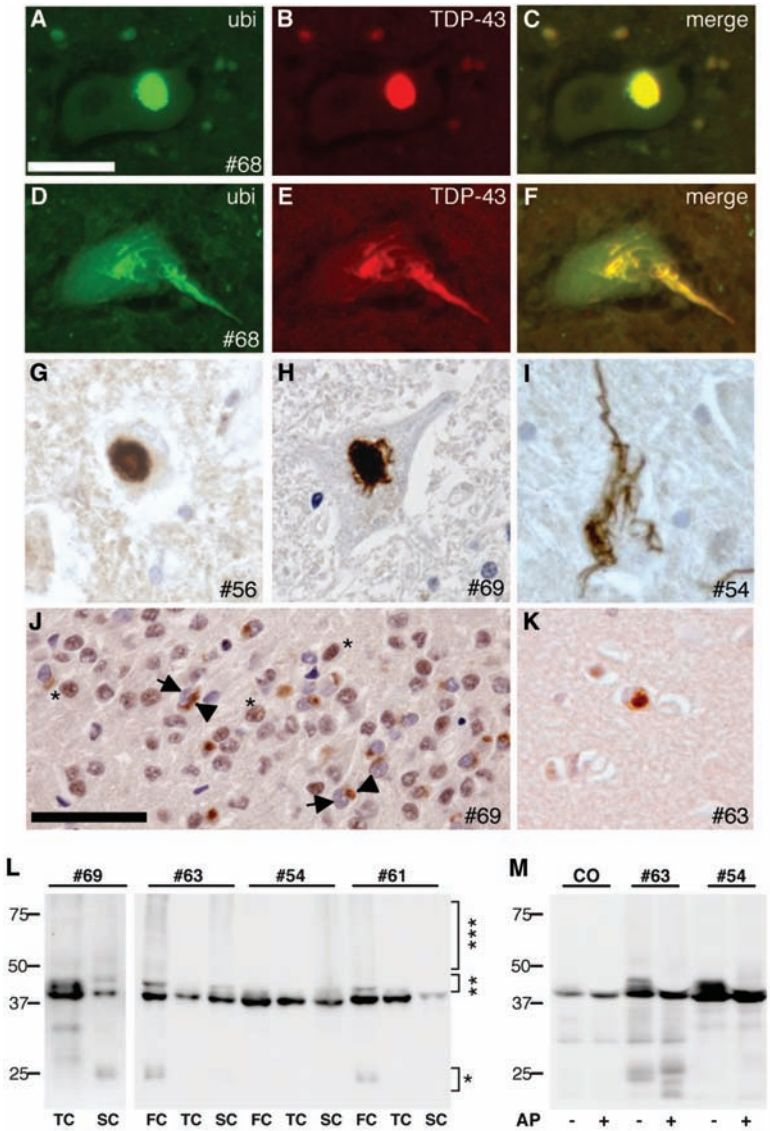

Fig. 4. UBIs in sporadic ALS were detected by anti–TDP-43. Double-label immunofluorescence with anti-ubiquitin (**A** and **D**) and anti–TDP-43 (**B** and **E**) showed colocalization in round (**C**) and skeinlike UBIs in spinal cord motor neuron (**F**). Merge images are shown in (C) and (F). Immunostaining with anti–TDP-43 labeled Lewy body–like (**G**), round (**H**), and skeinlike inclusions (**I**) in motor neurons of the spinal cord. Cytoplasmic UBIs in hippocampal dentate granule neurons (**J**) and few UBIs in frontal cortex (**K**) were also stained by TDP-43 (asterisk, normal nuclear staining; arrows, absence of nuclear staining in UBI-bearing neurons; arrowheads, UBIs). Scale bar in (A) corresponds to 25 μm [(A) to (I)]; scale bar in (J) corresponds to 50 μm [(J) and (K)]. (**L**) Immunoblots of urea fractions from frontal cortex (FC), temporal cortex (TC), and spinal cord (SC) of ALS cases probed with anti–TDP-43 demonstrated variable presence of the pathologic C-terminal fragments (*), 45-kD bands (**), and high M_r smear (***). (**M**) Immunoblots of dephosphorylated ALS urea extracts with anti–TDP-43 revealed collapse of the 45-kD band into the 43-kD band and increase in complexity of truncated TDP-43-immunoreactive bands ~23 to 27 kD.

abnormal hyperphosphorylation of TDP-43 might play a role in FTLD-U pathogenesis. Because UBIs are defined by ubiquitin immunohistochemistry, we asked whether TDP-43 recovered from urea fractions of FTLD-U brains is ubiquitinated, and this was shown to be the case by immunoprecipitation studies using the rabbit polyclonal anti–TDP-43 followed by immunoblot analyses with both anti–TDP-43 and ubiquitin antibodies (Fig. 3D).

FTLD-U and ALS have been suggested to be part of a clinicopathological spectrum (*23*), sharing similar pathogenic mechanisms that affect different populations of CNS neurons. We examined classic ALS cases for the presence of TDP-43–positive UBIs (table S1, nos. 54 to 72). Although none of the inclusions typical of ALS were detected by mAbs 182 and 406, all UBIs (including skeinlike, round, and Lewy body–like inclusions) in motor neurons of ALS were robustly double-labeled by TDP-43 and ubiquitin antibodies (Fig. 4, A to F) and by single-label TDP-43 immunohistochemistry (Fig. 4, G to I). A significant number of ALS patients demonstrate UBIs in hippocampus and frontal and temporal cortex (*23*), which were also immunolabeled by TDP-43 (Fig. 4, J and K).

Immunoblots of urea fractions of spinal cord as well as frontal and temporal cortices of ALS cases demonstrated a disease-specific signature for TDP-43 similar to that described above for FTLD-U (Fig. 4L). Dephosphoryation of the urea fractions showed that the 45-kD band in ALS corresponds to pathologically hyperphosphorylated TDP-43 as in FTLD-U (Fig. 4M). However, because the presence of UBIs in ALS cases is more variable than their presence in FTLD-U, not all brain regions examined in all cases exhibited pathological TDP-43.

These studies identify TDP-43 as the major disease protein in the signature UBIs of FTLD-U and ALS. Although pathologically altered TDP-43 proteins were present in all sporadic and familial FTLD-U as well as ALS cases, there were subtle differences in these abnormal TDP-43 variants among the three FTLD-U subtypes, which may be the result of similar but not identical pathogenic mechanisms. The differential distribution of UBIs detected by ubiquitin antibodies in FTLD-U subtypes (*18*) supports this view.

TDP-43 is a ubiquitously expressed, highly conserved nuclear protein (*24*) that may be a transcription repressor and an activator of exon skipping (*21*, *25*, *26*) as well as a scaffold for nuclear bodies through interactions with survival motor neuron protein (*27*). TDP-43 is normally localized primarily to the nucleus, but our data indicate that, under pathological conditions in FTLD-U, TDP-43 is eliminated from nuclei of UBI-bearing neurons, a consequence of which may be a loss of TDP-43 nuclear functions. Moreover, nuclear UBIs are rare in sporadic FTLD-U because most pathological TDP-43 accumulates in neuronal cell bodies or their processes, and it is unclear whether physiological TDP-43 is present at significant quantities in the cytoplasm, axons, and dendrites of normal neurons. Lastly, both FTDP-17U pedigrees examined here contain *PGRN* gene mutations (*11*), but the relation between TDP-43 and *PGRN*, which encodes a secreted growth factor involved in the regulation of multiple processes in development, wound repair, and inflammation (*28*), remains unclear.

The identification of TDP-43 as the major component of UBIs specific to sporadic and familial FTLD-U as well as sporadic ALS resolves a long-standing enigma concerning the nature of the ubiquitinated disease protein in these disorders. Thus, these diseases may represent a spectrum of disorders that share similar pathological mechanisms, culminating in the progressive degeneration of different selectively vulnerable neurons. These insights into the molecular pathology of FTLD-U and ALS can accelerate efforts to develop better therapies for these disorders.

References and Notes

1. M. S. Forman, J. Q. Trojanowski, V. M.-Y. Lee, *Nat. Med.* **10**, 1055 (2004).
2. J. R. Hodges *et al.*, *Ann. Neurol.* **56**, 399 (2004).
3. A. M. Lipton, C. L. White III, E. H. Bigio, *Acta Neuropathol.* (*Berlin*) **108**, 379 (2004).
4. J. K. Johnson *et al.*, *Arch. Neurol.* **62**, 925 (2005).
5. J. Shi *et al.*, *Acta Neuropathol.* (*Berlin*) **110**, 501 (2005).
6. M. S. Forman *et al.*, *Ann. Neurol.* **59**, 952 (2006).
7. G. M. McKhann *et al.*, *Arch. Neurol.* **58**, 1803 (2001).
8. M. Grossman, *J. Int. Neuropsychol. Soc.* **8**, 566 (2002).
9. D. Neary *et al.*, *Neurology* **51**, 1546 (1998).
10. C. Lomen-Hoerth, T. Anderson, B. Miller, *Neurology* **59**, 1077 (2002).
11. M. Baker *et al.*, *Nature* **442**, 916 (2006).
12. M. Cruts *et al.*, *Nature* **442**, 920 (2006).
13. P. Poorkaj *et al.*, *Ann. Neurol.* **43**, 815 (1998).
14. M. Hutton *et al.*, *Nature* **393**, 702 (1998).
15. R. Rademakers *et al.*, *Mol. Psychiatry* **7**, 1064 (2002).
16. I. R. Mackenzie *et al.*, *Brain* **129**, 853 (2006).
17. C. L. Lendon *et al.*, *Neurology* **50**, 1546 (1998).
18. D. M. Sampathu *et al.*, *Am. J. Pathol.*, in press.
19. Materials and methods are available as supporting material on *Science* Online.
20. S. H. Ou, F. Wu, D. Harrich, L. F. Garcia-Martinez, R. B. Gaynor, *J. Virol.* **69**, 3584 (1995).
21. E. Buratti *et al.*, *EMBO J.* **20**, 1774 (2001).
22. H. Y. Wang, I. F. Wang, J. Bose, C. K. Shen, *Genomics* **83**, 130 (2004).
23. I. R. Mackenzie, H. H. Feldman, *J. Neuropathol. Exp. Neurol.* **64**, 730 (2005).
24. Y. M. Ayala *et al.*, *J. Mol. Biol.* **348**, 575 (2005).
25. P. A. Mercado, Y. M. Ayala, M. Romano, E. Buratti, F. E. Baralle, *Nucleic Acids Res.* **33**, 6000 (2005).
26. E. Buratti, A. Brindisi, F. Pagani, F. E. Baralle, *Am. J. Hum. Genet.* **74**, 1322 (2004).
27. I. F. Wang, N. M. Reddy, C. K. Shen, *Proc. Natl. Acad. Sci. U.S.A.* **99**, 13583 (2002).
28. Z. He, A. Bateman, *J. Mol. Med.* **1**, 600 (2003).

29. We thank the Penn Proteomics Core Facility for the LC-MS/MS and M. Forman for critical comments on the manuscript. This work was funded by NIH (grants AG10124, AG17586, and T32 AG00255) and German Brain Bank "Brain-Net" (grant 01GI0299).

Supporting Online Material
www.sciencemag.org/cgi/content/full/314/5796/130/DC1
Material and Methods
Figs. S1 to S3
Table S1
References

21 August 2006; accepted 8 September 2006
10.1126/science.1134108

Infectious Prions in the Saliva and Blood of Deer with Chronic Wasting Disease

Candace K. Mathiason,[1] Jenny G. Powers,[3] Sallie J. Dahmes,[4] David A. Osborn,[5] Karl V. Miller,[5] Robert J. Warren,[5] Gary L. Mason,[1] Sheila A. Hays,[1] Jeanette Hayes-Klug,[1] Davis M. Seelig,[1] Margaret A. Wild,[3] Lisa L. Wolfe,[6] Terry R. Spraker,[1,2] Michael W. Miller,[6] Christina J. Sigurdson,[1] Glenn C. Telling,[7] Edward A. Hoover[1]*

A critical concern in the transmission of prion diseases, including chronic wasting disease (CWD) of cervids, is the potential presence of prions in body fluids. To address this issue directly, we exposed cohorts of CWD-naïve deer to saliva, blood, or urine and feces from CWD-positive deer. We found infectious prions capable of transmitting CWD in saliva (by the oral route) and in blood (by transfusion). The results help to explain the facile transmission of CWD among cervids and prompt caution concerning contact with body fluids in prion infections.

The prion diseases, or transmissible spongiform encephalopathies (TSEs), are chronic, degenerative, neurological diseases with uniformly fatal outcomes. TSEs are characterized by the conversion of the normal cellular prion protein (PrP^c) to an aberrant insoluble partially protease-resistant isoform (PrP^{res}). CWD, a transmissible spongiform encephalopathy of cervids (deer, elk, and moose), was first observed in the 1960s in captive deer and free-ranging deer and elk in northeastern Colorado and southeastern